Journal of Cerebral Blood Flow & Metabolism (2011) 31, 767–777

www.jcbfm.com

A dynamic *in vitro* BBB model for the study of immune cell trafficking into the central nervous system

Luca Cucullo[1,2], Nicola Marchi[1,2], Mohammed Hossain[1,2] and Damir Janigro[1,2,3]

[1]*Cerebrovascular Research, Cleveland Clinic Lerner College of Medicine, Cleveland, Ohio, USA;*
[2]*Department of Cell Biology, Cleveland Clinic Lerner College of Medicine, Cleveland, Ohio, USA;*
[3]*Department of Molecular Medicine, Cleveland Clinic Lerner College of Medicine, Cleveland, Ohio, USA*

Although there is significant evidence correlating overreacting or perhaps misguided immune cells and the blood–brain barrier (BBB) with the pathogenesis of neuroinflammatory diseases, the mechanisms by which they enter the brain are largely unknown. For this purpose, we revised our humanized dynamic *in vitro* BBB model (DIV-BBBr) to incorporate modified hollow fibers that now feature transmural microholes (2 to 4 μm $\varnothing$) allowing for the transendothelial trafficking of immune cells. As with the original model, this new DIV-BBBr reproduces most of the physiological characteristics of the BBB *in vivo*. Measurements of transendothelial electrical resistance (TEER), sucrose permeability, and BBB integrity during reversible osmotic disruption with mannitol (1.6 mol/L) showed that the microholes do not hamper the formation of a tight functional barrier. The *in vivo* rank permeability order of sucrose, phenytoin, and diazepam was successfully reproduced *in vitro*. Flow cessation followed by reperfusion (Fc/Rp) in the presence of circulating monocytes caused a biphasic BBB opening paralleled by a significant increase of proinflammatory cytokines and activated matrix metalloproteinases. We also observed abluminal extravasation of monocytes but only when the BBB was breached. In conclusion, the DIV-BBBr represents the most realistic *in vitro* system to study the immune cell trafficking across the BBB.
Journal of Cerebral Blood Flow & Metabolism (2011) **31,** 767–777; doi:10.1038/jcbfm.2010.162; published online 15 September 2010

Keywords: atherosclerosis; alternative; cerebral blood flow; inflammation; *in vitro*; ischemia; shear stress; white blood cells

Introduction

Transendothelial leukocyte migration across an altered brain microvascular bed is one of the most prominent features of many neuroimmune disorders; leukocytes are found in large numbers in the brain after trauma and certain neurodegenerative diseases. It is not clear whether the cells cross the endothelium through tight junctions, via a large pore or vacuole in the endothelial cell (EC), or through some other mechanism (Greenwood *et al*, 1994). This is a critical issue as increasing evidence indicates that inflammation and the blood–brain barrier (BBB) (Banks and Erickson, 2010; Lochhead *et al*, 2010) are involved in the pathogenesis of neurologic diseases such as meningitis (van der *et al*, 2004), brain edema (Stamatovic *et al*, 2006), Alzheimer's disease (Kalaria, 1992), and multiple sclerosis (Minagar and Alexander, 2003). Therefore, understanding the mechanisms of leukocyte trafficking into the brain might provide useful insights into how to modulate pathologic immune responses or enhance host protective mechanisms in neuroinflammatory diseases.

Locally secreted proinflammatory cytokines, for example, interleukin-6 (IL-6), tumor necrosis factor-α (TNF-α), and interleukin-1β (IL-1β) mediate the interactions between leukocytes and microvascular ECs. Vascular EC at the site of inflammation undergo a number of morphological and functional alterations, including increased BBB permeability, hypertrophy, accumulation of intracellular organelles, and proliferation (Cavender *et al*, 1989). For example, the exposure of endothelium to proinflammatory cytokines (TNF-α, IL-6, and IL-1β) interrupts the BBB by disorganizing cell–cell junctions, decreasing the brain solute barrier and enhancing leukocyte endothelial adhesion and migration.

Correspondence: Dr D Janigro, Department of Cell Biology, Cleveland Clinic Foundation, NB-20 LRI, 9500 Euclid Avenue, Cleveland, OH 44195, USA.
E-mail: janigrd@ccf.org
This work was supported by Alternative Research Development Foundation (ARDF) (to LC) and NIH-2RO1 HL51614, NIH-RO1 NS43284, and NIH-RO1 NS38195 (to DJ).
Received 19 May 2010; revised 10 August 2010; accepted 18 August 2010; published online 15 September 2010

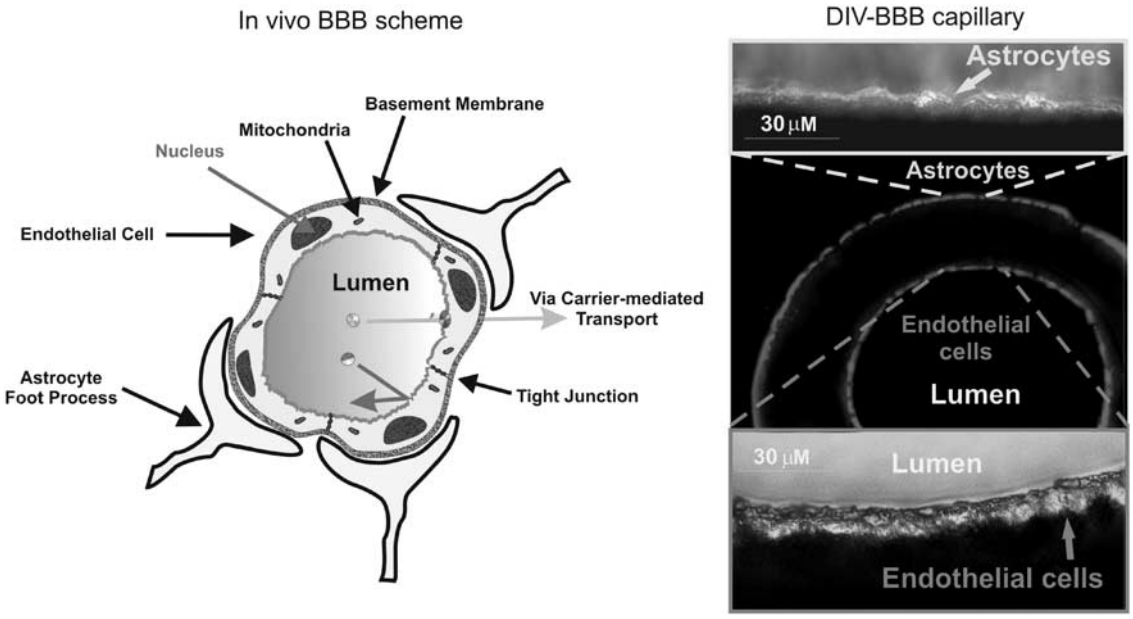

Figure 1 Cross-sectional view of artificial capillaries used in our model. Endothelial cells (ECs) cocultured with abluminal astrocytes in the dynamic *in vitro* blood–brain barrier (DIV-BBB) under flow condition develop a phenotype similar to that of the brain microvascular EC *in situ*.

Because of the lack of *in vitro* alternatives, *in vivo* models are by far the most widely used, to study the function of specific pathological mediators of neuroinflammatory disorders and their role in the pathogenesis and progression of the disease. Static *in vitro* devices such as the Transwell system lacks the physiological conditions (e.g., the presence of intraluminal flow), to maintain the phenotypic characteristics of the vascular endothelium *ex situ*. This has confined their use to basic linear kinetic studies of drug permeability, with limited translational significance in the clinical and pharmaceutical arenas. Furthermore, pathophysiological vascular changes such as hypoperfusion and ischemia (which represent a critical health issue for patients at risk of cardiovascular diseases) cannot be reproduced in this system. However, recent developments in the field have allowed for the establishment of *in vitro* brain vascular systems that overcome most of these limitations and provide a quasi-physiological environment where ECs and astrocytes can establish a functional BBB that closely mimics that *in vivo* (Cucullo *et al*, 2002, 2007; Salvetti *et al*, 2002; Parkinson *et al*, 2003; Krizanac-Bengez *et al*, 2006; Santaguida *et al*, 2006).

The use of hollow fiber technology has allowed the development of an artificial capillary system that provides a three-dimensional, fully controllable yet quasi-physiological environment where vascular ECs can be luminally exposed to physiological levels of flow and cocultured with abluminal astrocytes to form a functional BBB.

In this setting, the ECs exposed to pulsatile flow (which produces a pressure waveform comparable to the one *in vivo*; Cucullo *et al*, 2002) develop a phenotype similar to that of brain microvascular EC *in situ* (see Figure 1), which incorporates many of their physiological, anatomical, and biochemical characteristics, including metabolic and drug-resistant properties (Cucullo *et al*, 2002, 2007; Ghosh *et al*, 2010).

The dynamic *in vitro* (DIV)-BBB represents the most realistic *in vitro* system to study how hemodynamic changes and systemic inflammation affect the integrity of the brain microvasculature. However, the current model does not allow the transendothelial migration of immune cells. We now report that with the introduction of hollow fibers modified with larger transmural holes, we were able to overcome this problem without compromising the ability of the system to mimic the barrier properties. This represents a significant improvement of the model design that can greatly facilitate the study of endothelial–leukocyte interaction and the variety of mechanisms leading to immune cell extravasation into the brain. Furthermore, cells (from the BBB or circulating inside the capillary system) can be harvested, isolated, and analyzed by fluorescence activated cell sorting (FACS), cDNA arrays, or other means. This technology can be further expanded for the study of tumor cell extravasation into the brain parenchyma, which is a critical step in the pathogenesis of malignant brain tumors.

Materials and methods

Cell Culture

Normal adult human brain microvascular ECs (cat# 1000) and human adult astrocytes (cat# 1800) were purchased from ScienCell Research Laboratories, San Diego, CA,

USA. Human brain microvascular ECs were initially expanded in 75 cm^2 flasks precoated with fibronectin (3 $\mu g/cm^2$), with the appropriate endothelial growth medium consisting of MCDB 105 (Sigma, St Louis, MO, USA; Cat# M6395), 10% human AB serum (Sigma, Cat# S-7148), 15 mg/100 mL of EC growth supplement (Cat# 1052), 800 units/mL of heparin (Sigma, cat# H3393), 100 units/mL penicillin G sodium and 100 μg/mL streptomycin sulfate. Human adult astrocytes were grown in Poly-D-lysine precoated flasks (3 $\mu g/cm^2$) with Dulbecco's modified essential medium (F12) supplemented with 2 mmol/L glutamine, 5% fetal bovine serum, 100 units of penicillin G sodium per mL, and 100 μg of streptomycin sulfate per mL. All cells were maintained at 37°C in a humidified atmosphere with 5% CO_2. Cellular growth was monitored every day by inspection with phase contrast microscopy. Cell cultures were not passaged more than two times to minimize the dedifferentiation process.

The human monocytic leukemia cell line (THP-1, Cat# TIB-202) was purchased from American Type Culture Collection (Manassas, VA, USA). The THP-1 cells were grown at 37°C in 95% air to 5% CO_2 in basal medium (American Type Culture Collection-formulated RPMI-1640 Medium, Catalog No. 30-2001) plus 0.05 mmol/L 2-mercaptoethanol and 10% fetal bovine serum as specified by the vendor.

Dynamic *In Vitro* Blood–Brain Barrier Setup

Brain primary EC and astrocytes were cultured in the DIV-BBB, as previously described (Cucullo *et al*, 2002). Briefly, this iteration of the DIV-BBB consists of 11 hollow polypropylene fibers featuring larger transcapillary pores ($\varnothing \approx 2$ to 4 μm) inside a sealed chamber (the extraluminal space) accessible by ports. The fibers are connected in circuit with a media reservoir and a pulsatile pump apparatus through silicon gas-permeable tubing that allow for the exchange of O_2 and CO_2. The pump (CellMax QUAD Artificial Capillary Cell Culture System, Spectrum Laboratories Inc., Rancho Dominguez, CA, USA) can generate pulsatile flow rates ranging from 1 to 50 mL/min (corresponding to shear stress levels of $\sim$0.6 to 31.8 dyne/cm^2). In our experiments, we used a flow rate corresponding to a level of shear stress of 4 dyne/cm^2. The pulsatile nature of flow produces a pattern of intravascular perfusion comparable to physiological blood flow *in vivo* (Cucullo *et al*, 2002). The porosity of the hollow fibers allows gas and nutrient exchange between the luminal and the abluminal compartments but does not permit cells to cross. The luminal surface was precoated with 3 $\mu g/cm^2$ fibronectin (to allow for the adhesion of the ECs). The abluminal surface of the fibers was precoated using 3 $\mu g/cm^2$ of poly-D-lysine to allow for astrocytes adhesion.

Endothelial cells were first inoculated into the luminal compartment and allowed to adhere under static conditions over a 24-hour period. To achieve higher levels of cell attachment, the flow path was canalized through the extracapillary space for the same period of time. Astrocytes were seeded on the abluminal surface of the fibers 24 hours after the initial loading of the ECs. Following astrocytes seeding, the intraluminal flow was reestablished, and the vascular endothelium was initially exposed to a low-level shear stress (1 dyne/cm^2) for 24 hours. The shear stress was then gradually raised to physiological levels (4 dyne/cm^2) over the course of 7 days.

Transendothelial Electrical Resistance Measurement

The BBB integrity was monitored in real time by a transendothelial electrical resistance (TEER) measurement system, which uses electronic multiplexing to measure multiple cartridges in quick succession and assesses the integrity and viability of tissue culture bilayers rapidly and reliably (Cucullo *et al*, 2002; Santaguida *et al*, 2006). The device interfaces directly to a PC computer via Universal Serial Bus. Briefly, the system applies an excitation voltage (0.06 V) across the excitation electrodes inserted in each cartridge in the luminal and extraluminal compartments. The microcontroller computes the resistivity and capacitance per cm^2 of the barrier from physical parameters. The values of capacitance are calculated by comparison of the voltage and current waveforms. The delay from peak-to-peak of the two waveforms is proportional to the capacitance value, which is expressed as arch tension. The TEER was measured continuously from the initial setup throughout the course of each experiment. Previous work in our laboratory (McAllister *et al*, 2001; Santaguida *et al*, 2006; Cucullo *et al*, 2007) showed a direct (inverse) relationship between TEER and BBB permeability in the DIV-BBB.

Glucose Consumption and Lactate Production

The concentration of glucose and lactate in medium samples collected from intraluminal and the extraluminal was determined via a dual channel immobilized oxidase enzyme analyzer (YSI 2700 SELECT) and turntable (YSI Inc., Yellow Springs, OH, USA). Daily performance checks and assessment of the oxidase enzyme membrane integrity were performed according to the manufacturer's recommendations. The sampling protocol was set to recalibrate the machine every six samples as multiple samples were analyzed in the same run. Samples were kept frozen after being collected and processed at a later time, when multiple samples from the same experiment could be run simultaneously.

Cytokines and Matrix Metalloproteinases Measurement

Samples were taken from the luminal compartment, centrifuged at 5,000 *g* for 5 minutes and stored at −20°C until performing enzyme-linked immunosorbent assay. The biotinylated antibody reagent was added to 96-well enzyme-linked immunosorbent assay plate after the addition of the specific standards and experimental samples. After washing, the streptavidin–horseradish peroxidase complex is added for 30 minutes at room temperature, followed by tetra-methyl-benzidine and stop solution (1 mol/L sulfuric acid). Cytokine and matrix metalloproteinase (MMP) levels were then measured by an enzyme-linked immunosorbent assay plate reader at 450 to 550 nm.

Final concentrations were calculated taking into consideration the time of the measurement, as well as the total volume of the luminal compartment according to the following formula: $(V_t \times C_c) - (V_n \times C_n) + (V_{total} \times C_p)/T_c - T_p$, where V represents added volume of medium (mL); C refers to the concentration of certain cytokine/MMP level (pg/mL); T is time of sampling (in fraction of days: c and p indicate the current and previous samples, respectively; and n represents cytokine and MMP values in the fresh medium added after each sampling.

Matrix Metalloproteinase Activity

The MMP activity was assessed from the same samples using a specific MMP Gelatinase Activity Assay Kit (Chemicon ECM701, Billerica, MA, USA). Briefly, samples from the luminal compartment were centrifuged at 14,000 *g* for 15 minutes at 4°C to remove the cellular pellet. Total protein concentrations were determined on the supernatant by Bradford assay. Gelatin zymography was performed on 7.5% polyacrylamide gels copolymerized with 2 g/L 90 Bloom Type A gelatin from porcine skin (Sigma). After electrophoresis, gels were washed in Triton X-100 (25 mL/L) and incubated for 24 hours (37°C) in enzyme buffer (containing, per liter, 50 mmol of Tris-HCl, pH 7.5; 5 mmol of $CaCl_2$; 100 mmol of NaCl; 1 mmol of $ZnCl_2$; 0.2 g of Brij-35, Sigma-Aldrich, St Louis, MO, USA; 2.5 mL of Triton X-100; and 0.02 g of NaN_3). Finally, the gels were stained with 0.5% Coomasie Blue R-250. Gelatinolytic bands were measured densitometrically using Phoretix 2D software.

Blood–Brain Barrier Opening by Hyperosmolar Mannitol

Infusion of 2 mL of growth medium containing mannitol (1.6 mol/L) was used to open the BBB in the DIV-BBB apparatus according to previously reported methods (Rapoport, 2000). The mannitol solution was prepared under sterile conditions and injected intraluminally at a perfusion rate of 1 mL/min (total perfusion time was 120 seconds). The TEER was monitored during the course of the experiment to assess for BBB failure (= opening) and recovery. This was a clinical procedure that was used to facilitate the passage of chemotherapic drugs across the BBB into the central nervous system for the treatment of malignant brain tumors (Rapoport, 2000, 2001; Brown *et al*, 2004).

Statistical Analysis

For parametric variables (e.g., TEER levels, glucose consumption, lactate production cytokines levels), differences between populations were analyzed by analysis of variance. P values < 0.05 were considered statistically significant. Bonferroni analysis was used to account for comparisons of multiple parameters among groups. We used four cartridges/group. On the basis of the previous experiments, this number of cartridges provided sufficient power to demonstrate statistical significance for positive findings.

Results

Studies from this and other laboratories suggest that the main limitation of the model is its inability to allow for transendothelial cell trafficking between the vascular and the parenchymal compartment because of the diameter of the transcapillary pores (0.2 to 0.5 μm) of the hollow fibers. To address this problem, we have modified the original hollow fibers of the DIV-BBB system, which now accommodate transcapillary microholes (Figure 2A). This new

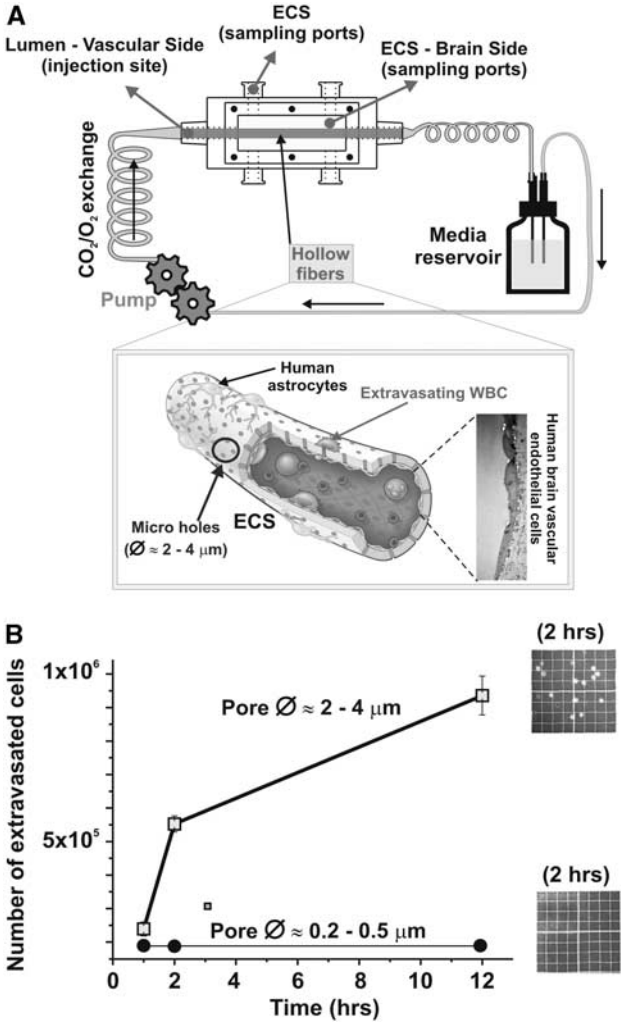

Figure 2 Schematic representation of the dynamic *in vitro* blood–brain barrier (DIV-BBB) model. (**A**) A bundle of porous polypropylene hollow fibers is suspended in the DIV-BBB chamber. The hollow fibers are in continuity with a medium source through a flow path consisting of gas-permeable silicon tubing. Note that the original hollow fibers have been modified to accommodate transcapillary microholes, which now make the artificial capillary permissive for cell extravasation (**B**). ECS, extraluminal space; WBC, white blood cells.

iteration of the DIV-BBB model is now permissive for the transendothelial trafficking of circulating THP-1 monocytes, which are a well characterized and widely used human acute monocytic leukemia cell line, with properties similar to that of human monocyte-derived macrophages. This is shown in Figure 2B, where THP-1 extravasation was observed only in DIV-BBB systems featuring the modified hollow fibers with transcapillary microholes of 2 to 4 μm of diameter. Extravasating cells can now be collected and analyzed (e.g., FACS, gene and protein arrays, etc).

Assessment of Blood–Brain Barrier Function and Integrity

A fundamental property of the BBB is the formation of an impediment to the passage of polar molecules and selective permeability to ions and other nutrients/substances. An index of this endothelial 'tightness' is the TEER (Stanness *et al*, 1997). In the first set of experiments to validate the model, we tested whether the presence of transcapillary microholes affected the establishment of a tight barrier. During the formation of the BBB (between the 8th and 18th day of coculture), the modules incorporating the original hollow fibers show a slight but statistically significant increase in resistance as indicated by the '*' symbols (Figure 3A, left panel, red plot). However, no significant differences were observed at later stage between TEER values achieved in the revised DIV-BBB (524 Ohm cm^2 ± s.e.m. 26.7) in comparison to the original unmodified system (573 Ohm cm^2 ± s.e.m. 28.9) (Figure 3A).

Functional assessment of the BBB was also evaluated by permeability measurements for the paracellular marker [^{14}C]-sucrose (3.16×10^{-6} cm/s ± s.e.m. 0.21) and other relevant compounds such as [^{14}C]-phenytoin (6.75×10^{-5} cm/s ± s.e.m. 0.38) or [^{14}C]-diazepam (6.88×10^{-3} cm/s ± s.e.m. 0.15) (Figure 3B). The dashed line (Figure 3C) indicates the idealized relationship if the *in vivo* data were identical to those *in vitro*. As demonstrated by the slope (S) values ($S = 0.85$), the new DIV-BBB model closely reproduced the *in vivo* rank order of permeabilities of sucrose, phenytoin, or diazepam (Patsalos *et al*, 1996; Walker *et al*, 1996). Furthermore, the low permeability to sucrose (3.16×10^{-6} cm/s ± s.e.m. 0.21) is consistent with the TEER measurements demonstrating the formation of a tight barrier. Note that the permeability was calculated by graphical integration of drug concentration in the lumen and in extraluminal space over 60 minutes. The integration protocol previously described by Cucullo *et al* (2007) and derived from a differential equation based on Fick's law reported elsewhere (Davson and Segal, 1996; Cucullo *et al*, 2007) removes the dimensional aspect of the calculation of permeability (μmol/L versus c.p.m.).

In conjunction with TEER monitoring and BBB permeability measurements, depletion of the main carbohydrate component of the growth medium (glucose) and accumulation of metabolically produced lactic acid are used as indicators of cell growth and differentiation (Stanness *et al*, 1996, 1997). Our results are shown in Figure 4A. Note that after a week of coculture in the DIV-BBB, lactate production/glucose consumption ratio reached a stable value ≈1 ± s.e.m. 0.11), indicating increased propensity toward an aerobic metabolic pattern as *in vivo*. In comparison, endothelial and glial cells cocultured in the absence of intraluminal flow showed a value ≈2 ± s.e.m. 0.14, which, as previously demonstrated, is indicative of a fully anaerobic metabolic behavior (Cucullo *et al*, 2002; Desai *et al*, 2002; Santaguida *et al*, 2006).

Intracarotid infusion of hyperosmolar (1.6 mol/L) mannitol, a cell impermeable and nontoxic polyalcohol, has been a useful tool for reversibly breaching the BBB *in vivo* and facilitate the passage of chemotherapic drugs during the treatment of metastatic or primary brain tumors (Rapoport, 2001). The DIV-BBBr system containing a monolayer of human BBB ECs grown under dynamic condition in the presence of extraluminal glial cells was intraluminally perfused (over 30 seconds), with hyperosmolar growth media containing mannitol (1.6 mol/L), and TEER was measured to assess real-time changes of BBB integrity (Figure 4B). Transient BBB disruption was successfully achieved in the new system and the duration of peak BBB opening was ≈35 minutes ± s.e.m. 5. This demonstrates that the new DIV-BBB mimics the physiological behavior of the BBB *in situ*.

The Dynamic *In Vitro* Blood–Brain Barrier to Study Immune Cell Extravasation into the Central Nervous System

Trafficking of immune cells across the BBB into the brain is a characteristic of many neuroinflammatory diseases. Severe hemodynamic changes such as flow cessation followed by reperfusion have been previously shown to induce vascular inflammation, endothelial–leukocyte interaction followed by a loss of BBB integrity and the extravasation of immune cells across the vascular endothelium and perhaps into the brain parenchyma (Huang *et al*, 2006; Jin *et al*, 2010).

Parallel new and conventional DIV-BBB modules were established (Figure 5A, left panel) to compare the effect of flow cessation/reperfusion on the integrity of the BBB. As shown in Figure 5A (right panel, highlighted yellow bar), 1 hour flow cessation followed by reperfusion (Fc/Rp,) in the presence of circulating THP-1 monocytes caused a biphasic opening of the BBB similar to that observed *in vivo* (Chen *et al*, 2009) in both the conventional and the new DIV-BBB systems. Note that the onset of BBB failure after reperfusion in the revised DIV-BBB initiated 1 hour earlier than in the conventional DIV-BBB. Furthermore, in the new DIV-BBB, the loss

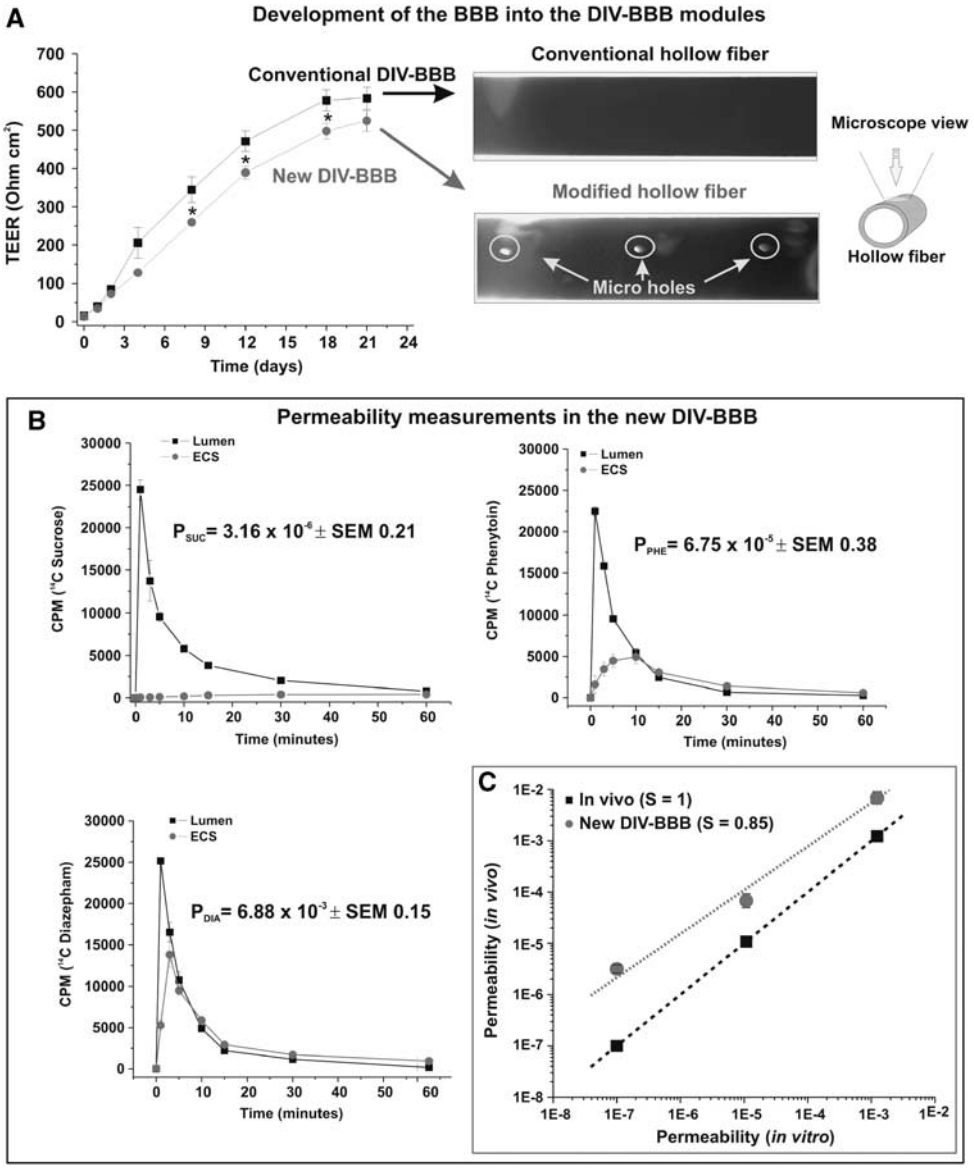

Figure 3 Development of a functional blood–brain barrier (BBB) in the new dynamic *in vitro* (DIV)-BBB system. (**A**) The presence of larger transcapillary pores in the revised DIV-BBB does not impact the process of formation of the integrity of the BBB measured by transendothelial electrical resistance. The asterisk indicates a non-statistically significant difference ($P > 0.05$) during the early stage of BBB formation in the new versus the conventional DIV-BBB. Note the microholes manufactured in the hollow fibers under transmitted light microscopy. (**B**) Permeability measurements to sucrose, phenytoin, and diazepam reflect the formation of a BBB capable of discriminating between solutes with different lipophilicity. Please note that the counts per minute (c.p.m.) versus time curves reflect the relative amount of solutes (expressed in c.p.m.) in the lumen and in the extraluminal space (ECS) at a given time point. (**C**) The dashed line indicates the idealized relationship if the data *in vivo* were identical to *in vitro*. Note how permeability obtained in the DIV-BBB closely mimic the *in vivo* scenario. TEER, transendothelial electrical resistance.

of BBB integrity during the second opening was 2 and half hours longer (± s.e.m. 25 minutes). Note also (Figure 5B) that the extravasation of immune cells was observed only in the new DIV-BBB featuring hollow fibers with transcapillary microholes and only in those systems undergoing Fc/Rp. In fact, no extravasation was observed in the absence of flow cessation/reperfusion. This suggests that the new DIV-BBB model can mimic the BBB *in situ* with respect to extravasation of monocytes.

Analysis of media samples taken 12 hours since reperfusion clearly show (relative to the corresponding controls) a substantial increase in the luminal medium level of IL-6 and TNF-α (Figure 6A) and that of MMP-2 and -9 as well (Figure 6B). The IL-1β levels were unaffected. No differences were observed between new and conventional modules. However, measurements of MMP-9 activity measured by zimography at 12 hours reperfusion (Figure 6C, right panel) was significantly higher in the samples

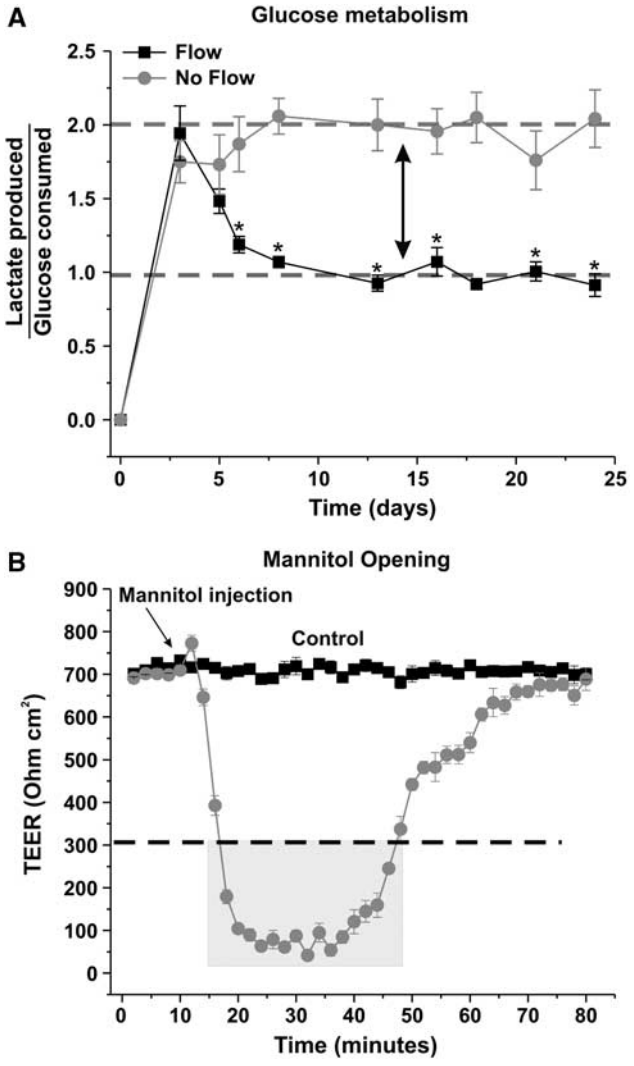

Figure 4 Functional characterization of the dynamic *in vitro* blood–brain barrier (DIV-BBB). (**A**) Under dynamic (flow) culture conditions, the ratio between glucose consumption and lactate production is ≈ 1. This indicates increased propensity toward an aerobic metabolic pattern, which is a well-established indicator of the formation of a functional BBB (Santaguida *et al*, 2006). The asterisk indicates a statistically significant difference ($P < 0.05$) versus parallel systems established under static conditions. (**B**) Hyperosmolar opening of the BBB in DIV models was assessed by real-time measurements of transendothelial electrical resistance (TEER). Similar to what was observed *in vivo*, the transient nature of the BBB opening is indicative of the formation of an *in vitro* BBB that closely mimic the physiological response of that *in situ*.

collected from the new DIV-BBB modules featuring larger transmural pores than that from the conventional ones. This is consistent with the TEER measurements shown in Figure 5A (right panel), demonstrating a higher degree of loss of BBB integrity in the new modules versus the conventional ones. In contrast to MMP-9, we observed only a modest trend for an increase in MMP-2 activity thus suggesting that MMP-9 has the major role in the loss of BBB integrity.

These findings show that (1) the newly designed DIV-BBB models reproduce the crucial features of the 'old' DIV-BBB; (2) the presence of transmural microholes, perhaps reducing the intrinsic resistance of the hollow fibers, allows for a more realistic assessment of the BBB opening caused by flow cessation reperfusion; and (3) as in our previous work, and shown repeatedly by others (Rosenberg *et al*, 1998), MMPs (and particularly MMP-9) are crucial players of postperfusion BBB damage.

Discussion

The burgeoning field of leukocyte trafficking has created new and exciting opportunities in clinical and translational research. Trafficking signals finely control the movement of distinct subsets of immune cells into and out of central nervous system (Johnson *et al*, 2007; Suidan *et al*, 2008). As the accumulation of leukocytes in the brain contributes to a wide variety of diseases, these 'molecular codes' have provided new targets for inhibiting tissue-specific inflammation, which have been confirmed clinically.

In vitro models are set to provide reliable cost-effective tools to facilitate these studies and accelerate the development, prescreening, and testing of novel therapeutic strategies to reduce the burden of these diseases. To this end, despite the numerous advantage of the DIV-BBB system versus conventional static models (Cucullo *et al*, 2005; Santaguida *et al*, 2006), the system is beset by its inability to realistically reproduce the transendothelial trafficking of immune cells because of the very small average diameter of the transcapillary pores (≈ 0.2 to $0.5\,\mu$m). For this purpose, we developed a novel DIV-BBB system based on the use of polypropylene hollow where larger transcapillary pores (≈ 2 to $4\,\mu$m in diameter) were manufactured by mechanical piercing (average density was 100 holes/cm^2 of capillary outer surface area). The main goal of this study was to validate this innovative revision of the DIV-BBB against the conventional (original) system (Cucullo *et al*, 2002).

Our results show that the presence of larger transcapillary pores does not affect the tightness of the BBB in fully established DIV-BBB system as demonstrated by TEER measurements and permeability to the paracellular marker sucrose. This demonstrates that differentiation of the vascular endothelium grown under uniform level of shear stress into a BBB phenotype is the main determinant for the establishment of a functional BBB *in vitro* and that this is not significantly affected by the properties of the supporting structure. Furthermore, the relationship between lipophilicity and permeability in the new DIV-BBB system was similar to that reported by others *in vivo* (Davson and Segal, 1996).

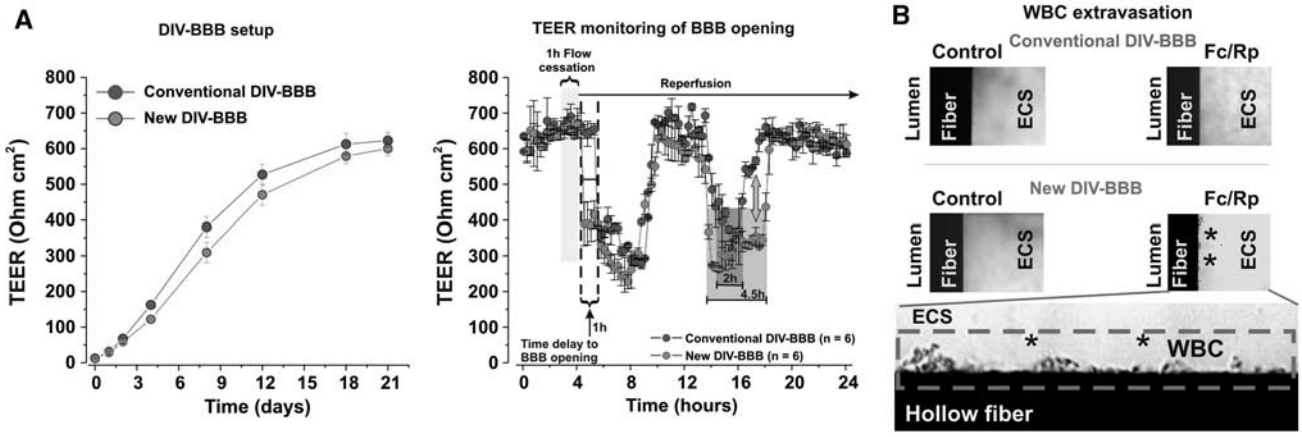

Figure 5 The new dynamic *in vitro* blood–brain barrier (DIV-BBB) model allows for the extravasation of monocytes when the BBB is breached. (**A**, left side) Transendothelial electrical resistance (TEER) measurements show the longitudinal progression of BBB formation in the conventional and new DIV-BBB used for the flow cessation reperfusion experiments. (**A**, right side) Flow cessation reperfusion (Fc/Rp, flow blockade for 1 hour) in the presence of circulating white blood cells causes a biphasic opening of the BBB. This loss of BBB integrity occurs earlier (1 hour) and is prolonged (2 hours) in the new DIV system where extravasation of cells is possible. Note that extravasation of monocytes into the abluminal (parenchymal) space occurs only when the DIV module featuring larger transcapillary pores was subjected to Fc/Rp (**B**). Monocytes, later identified by fluorescence activated cell sorting (FACS), are indicated with asterisk. No extravasation is observed in the traditional DIV-BBB model. These results suggest the possibility that an abluminal macrophagic action of activated monocytes may contribute to extend onset and duration of blood–brain barrier disruption (BBBD). ECS, extraluminal space; WBC, white blood cells.

The fact that the metabolic pattern of glucose consumption versus lactate production was identical to that observed in the original model (Santaguida *et al*, 2006) confirms that the revised DIV-BBB provides a culture environment in which ECs and astrocytes cocultured together develop BBB characteristics similar to that *in situ*. This is also in agreement with previous studies demonstrating that exposure to shear stress induces transcriptional changes at the genetic levels, which lead to the upregulation of the dehydrogenases and glyceraldehyde-3-phosphate dehydrogenase and the simultaneous decrease in lactate dehydrogenase (Desai *et al*, 2002). Both enzymes have a crucial role in the regulation of glucose metabolism and the regulation of the Krebs cycle. The formation of a transendothelial barrier was also demonstrated by restoration after transient loss of TEER caused by the exposure of the vascular endothelium to a hyperosmolar solution of mannitol. However, it is likely that in addition to ECs, glia shrinkage may also contribute to BBB changes, both *in vivo* and *in vitro*.

One of the most compelling reasons that prompted us to revise and improve the DIV-BBB system is the idea that by enabling transmural white blood cell (WBC) extravasation, we will be able to dissect the role played by the various subtypes of immune cells on BBB function and integrity in response to endogenous (and exogenous) proinflammatory stimuli. We previously demonstrated that in the DIV-BBB flow cessation/reperfusion in the presence of circulating WBC causes a biphasic loss of BBB integrity paralleled by a strong vascular inflammatory response similar to that observed *in situ* (Cucullo *et al*, 2008). Our results showed that the revised DIV-BBB provides a similar response to Fc/Rp and that, in addition to an often argued transcellular route, the loss of BBB integrity can provide a potential paracellular course for immune cells trafficking into the brain. It is important to acknowledge that for the experiments described herein we used only THP-1 monocytes, which is a well-characterized human acute monocytic leukemia cell line. It is possible that other subtypes of leukocytes (e.g., neutrophils) will behave differently. Future experiments will be conducted to characterize the pattern of extravasation of other subpopulation of WBC and compare our findings with *in vivo* data.

It is, however, important to underscore that this is the first *in vitro* model that allows studying cell extravasations under realistic perfusion pressures and shear stress levels. This further reaffirms the notion that the DIV-BBB, in its new implementation significantly expands the ability to mimic *in vitro* the physiological response of the brain capillaries *in situ*.

Similar to *in vivo*, the biphasic opening of the BBB caused by loss of intraluminal flow was paralleled by the release of proinflammatory cytokines such as IL-6 and TNF-α and the release and activation of MMPs such as MMP-2 and -9. However, the activity of MMP-9 measured in the new DIV-BBB system was significantly higher than that assessed in the original DIV-BBB. In parallel, the magnitude and the duration of the BBB opening after flow cessation/reperfusion was significantly increased in the new model in comparison to the conventional DIV-BBB. This is in agreement with the fact that the passage of monocytes and macrophages across the BBB requires

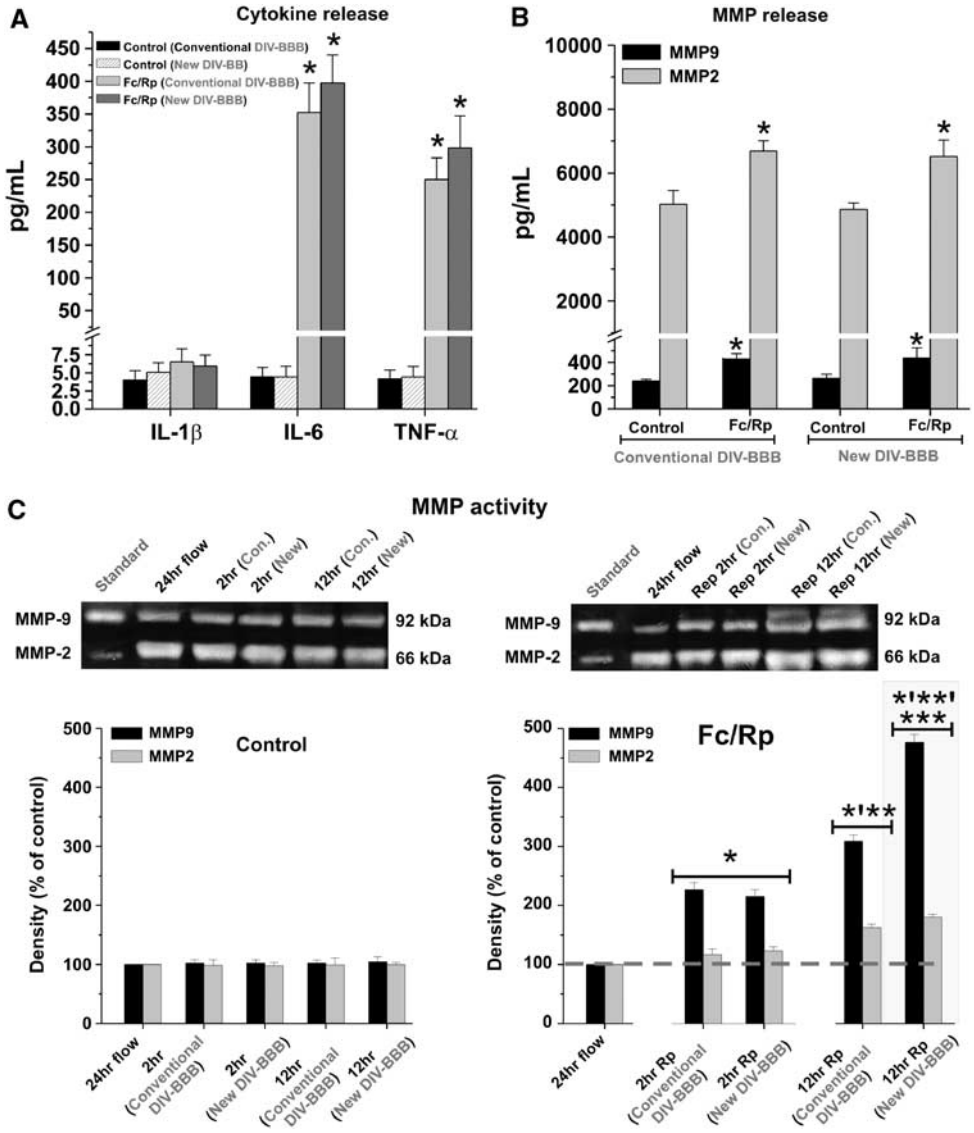

Figure 6 Effects of flow cessation reperfusion on blood–brain barrier (BBB) integrity are mediated by cytokines and matrix metalloproteinases (MMPs). (**A**) The loss of BBB integrity was paralleled by the release of the proinflammatory cytokines interleukin-6 (IL-6) and tumor necrosis factor α (TNF-α) as well as the release (**B**) and activation of MMP-2 and -9 (**C**). Note also that the activity level of MMP-9 measured in media samples from the new dynamic *in vitro* (DIV)-BBB system were significantly higher than that observed in the conventional model. The asterisk indicates a statistically significant difference ($P < 0.05$) versus controls. The double asterisk in panel C indicates a statistically significant difference ($P < 0.05$) between 2 and 12 hours postreperfusion corresponding to the occurrence of the second opening. The triple asterisk indicates a statistically significant difference ($P < 0.05$) between MMP-9 activity assessed in the new DIV-BBB system versus the conventional model.

MMP-9 activation (Sellebjerg and Sorensen, 2003). This hypothesis is also supported by the fact that in the absence of flow cessation, we did not observe WBC extravasation (Figure 5B) in the new DIV-BBB, and there was no difference in the level and activity of MMPs with the conventional model (Figure 6B).

Despite the fact that our revised DIV-BBB system is a very powerful model and represent one of the best possible approaches for studying leukocyte trafficking into the brain, we are aware of its limitations. The DIV-BBBr while consisting of several improvements compared with its predecessor, will not necessarily allow a full understanding of the mechanisms of leukocytes trafficking into the brain. This is because the model does not include all the elements of the brain environment. For example, neurons, microglia, oligodendrocytes, etc. are not included in the system. The three-dimensional structure of the hollow fiber provides a structural support to grow EC and abluminal astrocytes in a capillary-like manner. However, one of the differences between the anatomy of the vessels in the brain and those mimicked *in vitro* in the DIV-BBBr is the significantly larger thickness of the 'basal membrane,' which in our case is represented by the hollow fiber wall (150 μm). This may affect the extravasation/

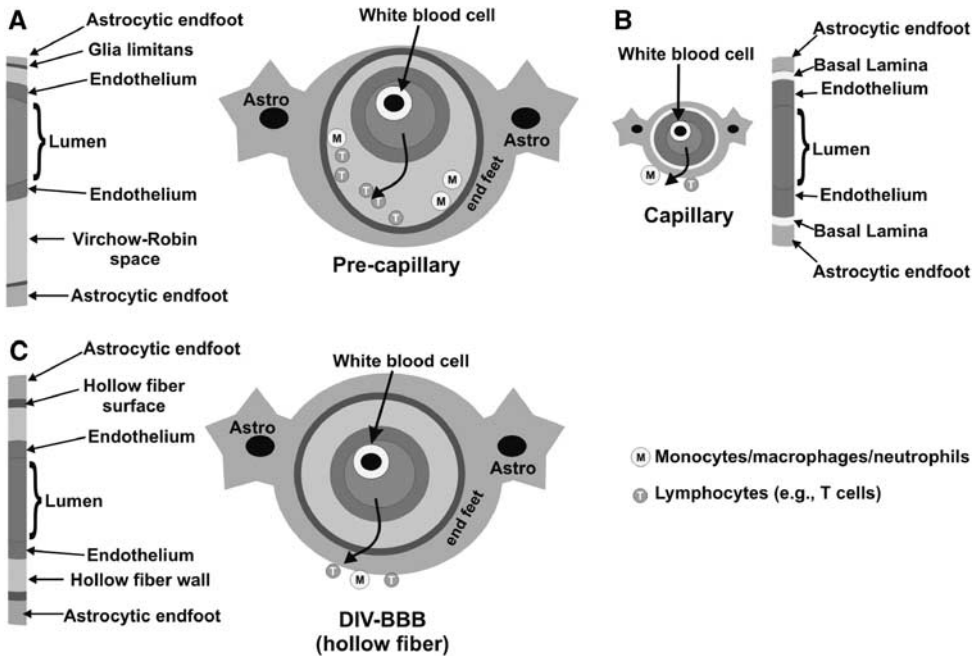

Figure 7 Schematic representation of capillary and postcapillary structure of the brain circulatory system in comparison to that of the dynamic *in vitro* blood–brain barrier (DIV-BBB). The figure shows a schematic representation of the cross-section of brain precapillary (**A**) and capillary (**B**) segments *in situ* and that of a hollow fiber used to manufacture the DIV-BBB (**C**). Note that the overall thickness of the hollow fibers (150 μm), which provide the support for endothelial cells and abluminal astrocytes is significantly larger than the basal lamina present at the endothelial–glia interface *in situ*. However, it is likely that the thickness of the hollow fiber interface is significantly reduced within the area of each microhole. Note also that the Virchow–Robin spaces that surround the precapillary segments are replaced by the hollow fiber wall, where the only empty space is represented by the transmural pores and microholes.

migration of the immune cells from the luminal compartment into the extraluminal space. Figure 7 shows the hypothetical pathway that WBC will encounter when extravasating *in vivo* or *in vitro*. Note that, in the model, there is an expansion of the space that separates the endothelium from the astrocytic layer on the abluminal surface of the hollow fibers. This is true whether we attempt to model the capillaries or the postcapillary segments. Under both circumstances, the hollow fibers support segregates endothelium from glia. We have noticed in an earlier work (Stanness *et al*, 1997) that glia endfeet protrude into the plastic support perhaps in an attempt to contact endothelia cells. We have no evidence that this happens in the present model, but given the presence of transmural microholes that was absent in the original system, we believe that it is likely that astrocytic endfeet contact ECs even under the present conditions.

In summary, the new DIV-BBB adds critical, yet unexploited, features to further increase the *in vivo* physiological connotation of the DIV brain vascular models. This will facilitate studying the pathological cues associated with the inflammatory response of the brain capillary and our understanding of the mechanisms regulating BBB functions and blood–brain trafficking. This might provide useful insights into how to modulate pathologic immune responses or enhance host protective mechanisms in neuroinflammatory diseases (Engelhardt and Ransohoff, 2005).

Disclosure/conflict of interest

Dr Janigro has the right to receive royalty payments for inventions or discoveries related to Flocel Inc. Dr Janigro owns stock or stock options of Flocel Inc. for activities as a founder, inventor, or consultant. Dr Cucullo owns stock or stock options of Flocel Inc. for activities as a founder or consultant. Dr Marchi owns stock or stock options of Flocel Inc. for activities as a scientific advisor.

References

Banks WA, Erickson MA (2010) The blood-brain barrier and immune function and dysfunction. *Neurobiol Dis* 37:26–32

Brown RC, Egleton RD, Davis TP (2004) Mannitol opening of the blood-brain barrier: regional variation in the permeability of sucrose, but not 86Rb+ or albumin. *Brain Res* 1014:221–7

Cavender DE, Edelbaum D, Ziff M (1989) Endothelial cell activation induced by tumor necrosis factor and lymphotoxin. *Am J Pathol* 134:551–60

Chen B, Friedman B, Cheng Q, Tsai P, Schim E, Kleinfeld D, Lyden PD (2009) Severe blood-brain barrier disruption and surrounding tissue injury. *Stroke* 40:e666–74

Cucullo L, Aumayr B, Rapp E, Janigro D (2005) Drug delivery and *in vitro* models of the blood-brain barrier. *Curr Opin Drug Discov Devel* 8:89–99

Cucullo L, Couraud PO, Weksler B, Romero IA, Hossain M, Rapp E, Janigro D (2008) Immortalized human brain endothelial cells and flow-based vascular modeling: a marriage of convenience for rational neurovascular studies. *J Cereb Blood Flow Metab* 28:312–28

Cucullo L, Hossain M, Rapp E, Manders T, Marchi N, Janigro D (2007) Development of a humanized *in vitro* blood-brain barrier model to screen for brain penetration of antiepileptic drugs. *Epilepsia* 48:505–16

Cucullo L, McAllister MS, Kight K, Krizanac-Bengez L, Marroni M, Mayberg MR, Stanness KA, Janigro D (2002) A new dynamic *in vitro* model for the multidimensional study of astrocyte-endothelial cell interactions at the blood-brain barrier. *Brain Res* 951:243–54

Davson H, Segal MB (1996) Blood-brain barrier. In: *Physiology of the CSF and blood–brain barriers* (Davson H, Segal MB, eds), Boca Raton, pp 49–91

Desai SY, Marroni M, Cucullo L, Krizanac-Bengez L, Mayberg MR, Hossain MT, Grant GG, Janigro D (2002) Mechanisms of endothelial survival under shear stress. *Endothelium* 9:89–102

Engelhardt B, Ransohoff RM (2005) The ins and outs of T-lymphocyte trafficking to the CNS: anatomical sites and molecular mechanisms. *Trends Immunol* 26:485–95

Ghosh C, Gonzalez-Martinez J, Hossain M, Cucullo L, Fazio V, Janigro D, Marchi N (2010) Pattern of P450 expression at the human blood-brain barrier: Roles of epileptic condition and laminar flow. *Epilepsia*; e-pub ahead of print

Greenwood J, Howes R, Lightman S (1994) The blood-retinal barrier in experimental autoimmune uveoretinitis. Leukocyte interactions and functional damage. *Lab Invest* 70:39–52

Huang J, Upadhyay UM, Tamargo RJ (2006) Inflammation in stroke and focal cerebral ischemia. *Surg Neurol* 66:232–45

Jin AY, Tuor UI, Rushforth D, Kaur J, Muller RN, Petterson JL, Boutry S, Barber PA (2010) Reduced blood brain barrier breakdown in P-selectin deficient mice following transient ischemic stroke: a future therapeutic target for treatment of stroke. *BMC Neurosci* 11:12

Johnson AJ, Suidan GL, McDole J, Pirko I (2007) The CD8 T cell in multiple sclerosis: suppressor cell or mediator of neuropathology? *Int Rev Neurobiol* 79:73–97

Kalaria RN (1992) The blood-brain barrier and cerebral microcirculation in Alzheimer disease. *Cerebrovasc Brain Metab Rev* 4:226–60

Krizanac-Bengez L, Mayberg MR, Cunningham E, Hossain M, Ponnampalam S, Parkinson FE, Janigro D (2006) Loss of shear stress induces leukocyte-mediated cytokine release and blood-brain barrier failure in dynamic *in vitro* blood-brain barrier model. *J Cell Physiol* 206:68–77

Lochhead JJ, McCaffrey G, Quigley CE, Finch J, Demarco KM, Nametz N, Davis TP (2010) Oxidative stress increases blood-brain barrier permeability and induces alterations in occludin during hypoxia-reoxygenation. *J Cereb Blood Flow Metab*; e-pub ahead of print

McAllister MS, Krizanac-Bengez L, Macchia F, Naftalin RJ, Pedley KC, Mayberg MR, Marroni M, Leaman S, Stanness KA, Janigro D (2001) Mechanisms of glucose transport at the blood-brain barrier: an *in vitro* study. *Brain Res* 904:20–30

Minagar A, Alexander JS (2003) Blood-brain barrier disruption in multiple sclerosis. *Mult Scler* 9:540–9

Parkinson FE, Friesen J, Krizanac-Bengez L, Janigro D (2003) Use of a three-dimensional *in vitro* model of the rat blood-brain barrier to assay nucleoside efflux from brain. *Brain Res* 980:233–41

Patsalos PN, O'Connell MT, Doheny HC, Sander JW, Shorvon SD (1996) Antiepileptic drug pharmacokinetics in patients with epilepsy using a new microdialysis probe: preliminary observations. *Acta Neurochir Suppl* 67:59–62

Rapoport SI (2000) Osmotic opening of the blood-brain barrier: principles, mechanism, and therapeutic applications. *Cell Mol Neurobiol* 20:217–30

Rapoport SI (2001) Advances in osmotic opening of the blood-brain barrier to enhance CNS chemotherapy. *Expert Opin Investig Drugs* 10:1809–18

Rosenberg GA, Estrada EY, Dencoff JE (1998) Matrix metalloproteinases and TIMPs are associated with blood-brain barrier opening after reperfusion in rat brain. *Stroke* 29:2189–95

Salvetti F, Cecchetti P, Janigro D, Lucacchini A, Benzi L, Martini C (2002) Insulin permeability across an *in vitro* dynamic model of endothelium. *Pharm Res* 19:445–50

Santaguida S, Janigro D, Hossain M, Oby E, Rapp E, Cucullo L (2006) Side by side comparison between dynamic versus static models of blood-brain barrier *in vitro*: a permeability study. *Brain Res* 1109:1–13

Sellebjerg F, Sorensen TL (2003) Chemokines and matrix metalloproteinase-9 in leukocyte recruitment to the central nervous system. *Brain Res Bull* 61:347–55

Stamatovic SM, Dimitrijevic OB, Keep RF, Andjelkovic AV (2006) Inflammation and brain edema: new insights into the role of chemokines and their receptors. *Acta Neurochir Suppl* 96:444–50

Stanness KA, Guatteo E, Janigro D (1996) A dynamic model of the blood-brain barrier '*in vitro*'. *Neurotoxicology* 17:481–96

Stanness KA, Westrum LE, Fornaciari E, Mascagni P, Nelson JA, Stenglein SG, Myers T, Janigro D (1997) Morphological and functional characterization of an *in vitro* blood-brain barrier model. *Brain Res* 771:329–42

Suidan GL, McDole JR, Chen Y, Pirko I, Johnson AJ (2008) Induction of blood brain barrier tight junction protein alterations by CD8 T cells. *PLoS One* 3:e3037

van der FM, Hoppenreijs S, van Rensburg AJ, Ruyken M, Kolk AH, Springer P, Hoepelman AI, Geelen SP, Kimpen JL, Schoeman JF (2004) Vascular endothelial growth factor and blood-brain barrier disruption in tuberculous meningitis. *Pediatr Infect Dis J* 23:608–13

Walker MC, Alavijeh MS, Shorvon SD, Patsalos PN (1996) Microdialysis study of the neuropharmacokinetics of phenytoin in rat hippocampus and frontal cortex. *Epilepsia* 37:421–7